Sidewall Carboxylic Acid Functionalization of Single-Walled Carbon Nanotubes

ARTICLE *in* JOURNAL OF THE AMERICAN CHEMICAL SOCIETY · JANUARY 2004

Impact Factor: 12.11 · DOI: 10.1021/ja037746s · Source: PubMed

4 AUTHORS, INCLUDING:

Valery N Khabashesku
Rice University
106 PUBLICATIONS **3,603** CITATIONS

SEE PROFILE

J|A|C|S
ARTICLES
Published on Web 11/15/2003

Sidewall Carboxylic Acid Functionalization of Single-Walled Carbon Nanotubes

Haiqing Peng, Lawrence B. Alemany, John L. Margrave,* and Valery N. Khabashesku*

Contribution from the Department of Chemistry and the Center for Nanoscale Science and Technology, Rice University, 6100 Main Street, Houston, Texas 77005-1892

Received August 4, 2003; E-mail: khval@rice.edu

Abstract: The reactions of single-walled carbon nanotubes (SWNTs) with succinic or glutaric acid acyl peroxides in *o*-dichlorobenzene at 80−90 °C resulted in the addition of 2-carboxyethyl or 3-carboxypropyl groups, respectively, to the sidewalls of the SWNT. These acid-functionalized SWNTs were converted to acid chlorides by derivatization with $SOCl_2$ and then to amides with terminal diamines such as ethylenediamine, 4,4′-methylenebis(cyclohexylamine), and diethyltoluenediamine. The acid-functionalized SWNTs and the amide derivatives were characterized by a set of materials characterization methods including attenuated total reflectance (ATR) FTIR, Raman and solid state ^{13}C NMR spectroscopy, transmission electron microscopy (TEM), and thermal gravimetry-mass spectrometry (TG-MS). The degree of SWNT sidewall functionalization with the acid-terminated groups was estimated as 1 in 24 carbons on the basis of TG-MS data. In comparison with the pristine SWNTs, the acid-functionalized SWNTs show an improved solubility in polar solvents, for example, alcohols and water, which enables their processing for incorporation into polymer composite structures as well as for a variety of biomedical applications.

Introduction

Since their discovery in 1993,[1] single-walled carbon nanotubes (SWNTs) have become an area of wide ranging research activity due to their exceptional chemical and physical properties. To take advantage of the remarkable tubular framework structure of SWNTs in various applications, particularly in the engineering of multifunctional materials, the SWNTs need to be derivatized with organic functional groups that can provide a high binding affinity and selectivity through formation of either hydrogen or covalent bonds. For medical and biological applications, the SWNTs must be chemically derivatized with hydrophilic substituents, such as those containing terminal hydroxyl or carboxylic acid groups. These functional groups are also necessary for providing sites for covalent integration of the SWNTs into organic/inorganic polymer structures to produce nanotube-reinforced composite materials.[2]

In addition to trying to meet these technological demands, the development of functionalization methods for nanotubes is also of fundamental importance for gaining a greater knowledge of chemical reactivity for materials with nanoscale size and shape. However, in light of the most recent reviews,[3] the number of documented studies in this new research field of functionalization chemistry of carbon nanotubes is not yet substantial. Reports have appeared of SWNT sidewall functionalizations using fluorine,[4] followed by subsequent interactions with alkyllithium[5] and Grignard[3c,f] reagents or diamines,[6] and reactions of SWNTs with aryl diazonium salts,[7] azomethine ylides,[8] nitrenes,[9] and organic radicals.[9−11] The SWNT open-end functionalizations have been most extensively explored through oxidation routes[3d,e,12,13] to form shortened nanotubes bearing carboxylic acid end groups that have been further derivatized

(1) (a) Iijima, S.; Ichihashi, T. *Nature* **1993**, *363*, 603. (b) Bethune, D. S.; Kiang, C. H.; de Vries, M. S.; Gorman, G.; Savoy, R.; Vazquez, J.; Beyers, R. *Nature* **1993**, *363*, 605.
(2) Zhu, J.; Kim, J.; Peng, H.; Margrave, J. L.; Khabashesku, V. N.; Barrera, E. V. *Nano Lett.* **2003**, *3*, 1107 and references therein.
(3) (a) Hirsch, A. *Angew. Chem., Int. Ed.* **2002**, *41*, 1853. (b) Bahr, J. L.; Tour, J. M. *J. Mater. Chem.* **2002**, *12*, 1952. (c) Khabashesku, V. N.; Billups, W. E.; Margrave, J. L. *Acc. Chem. Res.* **2002**, *35*, 1087. (d) Sun, Y.-P.; Fu, K.; Lin, Y.; Huang, W. *Acc. Chem. Res.* **2002**, *35*, 1096. (e) Niyogi, S.; Hamon, M. A.; Hu, H.; Zhao, B.; Bhowmik, P.; Sen, R.; Itkis, M. E.; Haddon, R. C. *Acc. Chem. Res.* **2002**, *35*, 1105. (f) Khabashesku, V. N.; Margrave, J. L. Chemistry of Carbon Nanotubes. In *The Encyclopedia of Nanoscience and Nanotechnology*; Nalwa, S., Ed.; American Scientific Publ.: Steveson Ranch, 2003. (g) Banerjee, S.; Wong, S. S. *J. Phys. Chem. B* **2002**, *106*, 12144.
(4) Mickelson, E. T.; Huffman, C. B.; Rinzler, A. G.; Smalley, R. E.; Hauge, R. H.; Margrave, J. L. *Chem. Phys. Lett.* **1998**, *296*, 188.
(5) (a) Boul, P. J.; Liu, J.; Mickelson, E. T.; Huffman, C. B.; Ericson, L. M.; Chiang, I. W.; Smith, K. A.; Colbert, D. T.; Hauge, R. H.; Margrave, J. L.; Smalley, R. E. *Chem. Phys. Lett.* **1999**, *310*, 367. (b) Saini, R. K.; Chiang, I. W.; Peng, H.; Smalley, R. E.; Billups, W. E.; Hauge, R. H.; Margrave, J. L. *J. Am. Chem. Soc.* **2003**, *125*, 3617.
(6) Stevens, J. L.; Huang, A. Y.; Peng, H.; Chiang, I. W.; Khabashesku, V. N.; Margrave, J. L. *Nano Lett.* **2003**, *3*, 331.
(7) Bahr, J. L.; Yang, J.; Kosynkin, D. V.; Bronikowski, M. J.; Smalley, R. E.; Tour, J. M. *J. Am. Chem. Soc.* **2001**, *123*, 6536.
(8) (a) Georgakilas, V.; Kordatos, K.; Prato, M.; Guldi, D. M.; Holzinger, M.; Hirsch, A. *J. Am. Chem. Soc.* **2002**, *124*, 760. (b) Georgakilas, V.; Tagmatarchis, N.; Pantarotto, D.; Bianco, A.; Briand, J.-P.; Prato, M. *Chem. Commun.* **2002**, 3050. (c) Pantarotto, D.; Partidos, C. D.; Graff, R.; Hoebeke, J.; Briand, J.-P.; Prato, M.; Bianco, A. *J. Am. Chem. Soc.* **2003**, *125*, 6160.
(9) (a) Holzinger, M.; Vostrowsky, O.; Hirsch, A.; Hennrich, F.; Kappes, M.; Weiss, R.; Jellen, F. *Angew. Chem., Int. Ed.* **2001**, *40*, 4002. (b) Holzinger, M.; Abraham, J.; Whelan, P.; Graupner, R.; Ley, L.; Hennrich, F.; Kappes, M.; Hirsch, A. *J. Am. Chem. Soc.* **2003**, *125*, 8566.
(10) Peng, H.; Reverdy, P.; Khabashesku, V. N.; Margrave, J. L. *Chem. Commun.* **2003**, 362.
(11) Ying, Y.; Saini, R. K.; Liang, F.; Sadana, A. K.; Billups, W. E. *Org. Lett.* **2003**, *5*, 1471.
(12) Banerjee, S.; Wong, S. S. *Nano Lett.* **2002**, *2*, 49.

10.1021/ja037746s CCC: $25.00

Scheme 1. Chemical Routes for Preparation of SWNT-Derivatives **2a** and **2b**

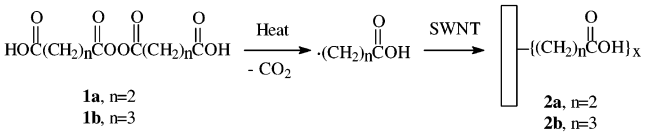

by reactions with thionyl chloride and long-chain amines[13,14] or by esterification.[15]

Until now, the most successful functionalization of carbon nanomaterials with carboxylic acid-terminated moieties has been with fullerene C_{60} through a two-step process (Bingel 2+1 cycloaddition reaction followed by deesterification) yielding carboxylated methanofullerene structures.[16] A similar process was shown to be much less efficient when applied to pristine SWNTs because of their reduced reactivity to carbene addition via a Bingel-type reaction.[17] With carbon nanotubes, the carboxylic acid functions have been generated so far only on their open ends and to some extent on the partially etched ("unzipped") sidewalls through treatment with various oxidants.[3]

In the present work, we demonstrate a one-step method for derivatization of SWNTs that is based on free radical addition of alkyl groups terminated with a carboxylic acid. This method, which is nondestructive to the sidewall, utilizes the organic acyl peroxides of dicarboxylic acids, $HOOC(CH_2)_nC(O)OO(O)C-(CH_2)_nCOOH$ (**1a**, $n = 2$; **1b**, $n = 3$), as precursors for the corresponding "functional" radicals. These precursors were chosen on the basis both of the well-known, long time use of peroxides as radical initiators in polymerization reactions and also of our successful sidewall functionalization of SWNTs by addition of alkyl or phenyl radicals thermally generated from organic acyl peroxides[10] (later confirmed by Ying et al.[11]). As compared to other radical sources, organic peroxides can offer more kinds of functional groups and are more conveniently available at relatively lower costs. Acyl peroxides, RC(O)OO-(O)CR, where R could be aliphatic, aromatic, or another group, readily decompose to release carbon dioxide and form free radicals R upon mild heating.[18] Succinic acid peroxide, **1a**, decomposes to form a $HOOCCH_2CH_2COO\cdot$ radical,[19−21] which can subsequently lose CO_2 to yield a 2-carboxyethyl radical. Glutaric acid peroxide, **1b**, would be expected to yield a 3-carboxypropyl radical via a similar route. In the present study, these carboxyalkyl radicals, generated in situ from peroxides **1a** and **1b**, have reacted with the SWNTs to produce sidewall acid-functionalized SWNT-derivatives **2a** and **2b**, respectively (Scheme 1).

Scheme 2. Preparation of SWNT Amide Derivative **3**

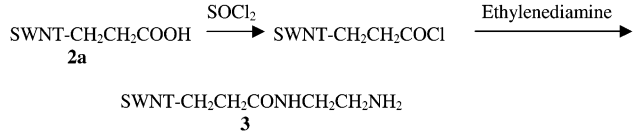

Scheme 3. Preparation of SWNT Amide Derivative **4**

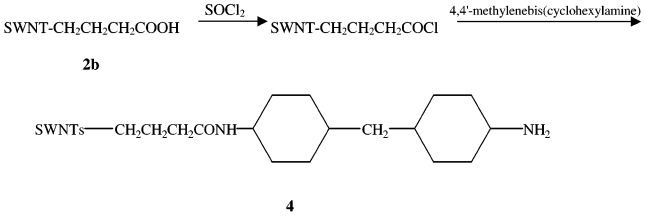

Scheme 4. Preparation of SWNT Amide Derivative **5**

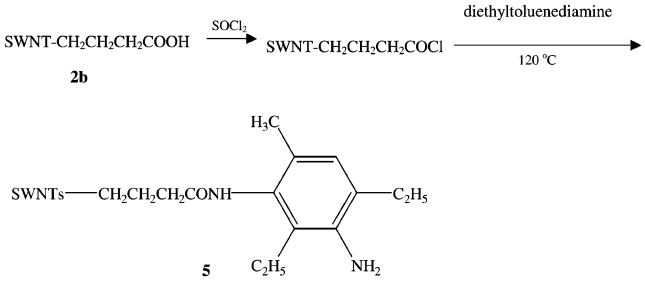

The attached carboxylic acid groups in **2a** and **2b** have been chemically characterized by formation of amide derivatives in the course of subsequent reactions with thionyl chloride and then with several terminal diamines, such as ethylenediamine, 4,4′-methylenebis(cyclohexylamine), and diethyltoluenediamine (Schemes 2−4). Instrumental analyses of the sidewall-functionalized SWNTs **2a**,**b** and their amide derivatives have been carried out with the help of both now commonly used optical spectroscopy and microscopy methods[3] as well as solid state ^{13}C NMR spectroscopy and thermal gravimetry-mass spectroscopy. The present paper provides a detailed discussion of these data.

Experimental Section

Materials. The raw SWNTs used in this study were produced by the HiPco process in Professor Richard Smalley's Carbon Nanotechnology laboratory at Rice University. Such prepared HiPco SWNTs have an average diameter of 1 nm. The iron impurity in the HiPco SWNTs was removed by wet air oxidation and subsequent hydrochloric acid rinse as described previously.[22] The final purification step was the annealing of the SWNTs at 800 °C in an argon atmosphere for 2 h. The iron residue in the purified SWNTs was found by TGA to be about 1 wt %. The SEM/EDX analysis yielded 0.2 at. % iron content in the same material.

Succinic and glutaric anhydrides, used as precursors for the preparation of dicarboxylic acid acyl peroxides, and ethylenediamine were purchased from Aldrich. 4,4′-Methylenebis(cyclohexylamine) was

(13) (a) Chen, J.; Hamon, M. A.; Hu, H.; Chen, Y.; Rao, A. M.; Eklund, P. C.; Haddon, R. C. *Science* **1998**, *282*, 95. (b) Hamon, M. A.; Chen, J.; Hu, H.; Chen, Y.; Itkis, M. E.; Rao, A. M.; Eklund, P. C.; Haddon, R. C. *Adv. Mater*. **1999**, *11*, 834.
(14) Liu, J.; Rinzler, A. G.; Dai, H.; Hafner, J. H.; Bradley, R. K.; Boul, P. J.; Lu, A.; Iverson, T.; Shelimov, K.; Huffman, C. B.; Rodriguez-Macias, F.; Shon, Y.-S.; Lee, T. R.; Colbert, D. T.; Smalley, R. E. *Science* **1998**, *280*, 1253.
(15) (a) Riggs, J. E.; Guo, Z.; Carroll, D. L.; Sun, Y.-P. *J. Am. Chem. Soc.* **2000**, *122*, 5879. (b) Sun, Y.-P.; Huang, W.; Lin, Y.; Fu, K.; Kitaygorodskiy, A.; Riddle, L. A.; Yu, Y. J.; Carroll, D. L. *Chem. Mater*. **2001**, *13*, 2864.
(16) (a) Lamparth, I.; Hirsch, A. *J. Chem. Soc., Chem. Commun.* **1994**, 1727. (b) Hirsch, A.; Lamparth, I.; Karfunkel, H. R. *Angew. Chem., Int. Ed. Engl.* **1994**, *33*, 437.
(17) (a) Kini, V. U.; Khabashesku, V. N.; Margrave, J. L. *Rice Quantum Institute Sixteenth Annual Summer Research Colloquium;* August 9, 2002; Abstr. p 25. (b) Coleman, K. S.; Bailey, S. R.; Fogden, S.; Green, M. L. H. *J. Am. Chem. Soc.* **2003**, *125*, 8722.
(18) *Organic Peroxides*; Swern, D., Ed.; Wiley-Interscience: New York, London, Sydney, Toronto, 1971; Vol. II, p 799.
(19) Fieser, L. F.; Turner, R. B. *J. Am. Chem. Soc.* **1947**, *69*, 2338.
(20) Pettit, G. R.; Houghton, L. E. *J. Chem. Soc. C* **1971**, 509.
(21) Anufriev, V. P.; Novikov, V. L.; Maximov, O. B.; Elyakov, G. B.; Levitsky, D. O.; Lebedev, A. V.; Sadretdinov, S. M.; Shvilkin, A. V.; Afonskaya, N. I.; Ruda, M. Y.; Cherpachenko, N. M. *Bioorg. Med. Chem. Lett.* **1998**, *8*, 587.
(22) Chiang, I. W.; Brinson, B. E.; Huang, A. Y.; Willis, P. A.; Bronikowski, M. J.; Margrave, J. L.; Smalley, R. E.; Hauge, R. H. *J. Phys. Chem. B* **2001**, *105*, 8297.

supplied by Air Products, and diethyltoluenediamine was purchased from Resolution Performance Products.

Synthetic Procedures. To prepare succinic and glutaric acid acyl peroxides (**1a** and **1b**), 10 g of succinic or glutaric anhydride fine powder was added to 20 mL of ice cold 8% hydrogen peroxide and stirred for 30 min until all of the powder dissolved and a white gellike solution formed. The solution was filtered onto a 1-μm pore size PTFE membrane (Cole Palmer) to leave a deposit which was washed with a small amount of water and air-dried for 10 min. The white peroxide products were transferred from the membrane to a glass vial and vacuum-dried at room temperature for 24 h. Approximately 6.5 g of each peroxide, **1a** and **1b**, was obtained using this one-step procedure reported long ago by Clover et al.[23] ATR-FTIR spectra of both peroxides **1a** and **1b** show similar features: a broad band in the 3000−3500 cm^{-1} region due to the carboxylic O−H stretches, peaks of the C−H stretchings in the 2850−3000 cm^{-1} range, absorptions near 1700 cm^{-1} characteristic of the acid carbonyl groups, and pairs of peaks at 1812 and 1779 cm^{-1} assigned to the peroxide carbonyls. The solid state ^{13}C NMR spectrum of **1a** shows three methylene carbon peaks at 29.9, 28.8, and 24.7 ppm and three carbonyl carbon peaks at 181.7, 179.7, and 168.7 ppm. The spectrum of **1b** shows three methylene peaks at 33.0, 28.4, and 19.0 ppm and two carbonyl peaks at 182.2 and 170.3 ppm.

To prepare acid-functionalized SWNTs (**2a** and **2b**), the following procedure was developed. Purified SWNTs (50 mg) were placed in a 250-mL flask filled with 50 mL of dry *o*-dichlorobenzene and sonicated (17 W/55 kHz bath, Cole Palmer) for 30 min to obtain a SWNT suspension solution. The latter was heated at 80−90 °C for 10 days while each day 0.5 g of peroxide **1a** or **1b** was added. After the reaction was complete, the suspension was cooled and poured into a 500-mL Erlenmeyer flask containing a large amount of tetrahydrofuran and sonicated for 15 min. The obtained solution was filtered using a 0.2-μm pore size PTFE membrane (Cole Palmer). Functionalized SWNTs **2a** or **2b**, respectively, were collected on the membrane, then placed in 100 mL of ethanol, sonicated for 20 min, and then filtered again. During the filtration, a large amount of ethanol was repeatedly used to completely wash off the unreacted peroxides and the reaction byproducts. Finally, the functionalized SWNTs **2a** and **2b** were vacuum-dried at 70 °C overnight.

The SWNT amide derivative **3** (Scheme 2) was prepared from 20 mg of acid-functionalized SWNT **2a** placed in a dry 100-mL flask to which 20 mL of thionyl chloride was added, and the mixture was stirred for 12 h. The reaction mixture was then vacuum filtered through a 0.2-μm pore size membrane, and the obtained precipitate was flushed with a large amount of dry acetone. The solid precipitate was dried in air and then placed in a 100-mL flask containing 20 mL of ethylenediamine. The mixture was stirred at room temperature for 12 h and then poured into a large amount of ethanol and sonicated for another 10 min. The batch was filtered through a 0.2-μm pore size membrane and flushed with a large amount of ethanol. The SWNT-derivative **3** was collected on a membrane and dried overnight in a vacuum oven at 70 °C. A similar procedure was applied for preparation of amide **4** (Scheme 3) by treating **2b** with $SOCl_2$ and 4,4′-methylenebis(cyclohexylamine). Unlike the syntheses of **3** and **4** at room temperature, the synthesis of amide derivative **5** from **2b** required heating at 120 °C for 12 h during the reaction with diethyltoluenediamine (Scheme 4).

Characterization. The Raman spectra of purified and functionalized SWNTs were collected with a Renishaw 1000 microraman system with a 780-nm laser source. For the ATR-FTIR spectral measurements, a Thermo Nicolet Nexus 870 FTIR system with an ATR accessory was employed. The spectra in the UV−vis−NIR range were taken using a Shimadzu 3101 PC UV/Vis/NIR spectrometer. The thermal degradation and volatile products evolution analyses were performed with a TGA/MS instrument which includes a Q500 Thermal Gravity Analyzer coupled with a Pffeifer Thermal Star mass spectrometer.

The solid state, magic angle spinning (MAS) NMR studies were done on a Bruker AVANCE-200 NMR spectrometer (50.3 MHz ^{13}C, 200.1 MHz ^{1}H). MAS spectra were obtained with each sample packed in a 4-mm outer diameter rotor, which was spun at 7.5 kHz for the pristine SWNTs and at 11.0 kHz for the functionalized SWNTs. This results in spinning sidebands well outside the sp^2 and sp^3 centerband regions of interest (149 ppm upfield or downfield from the centerband for pristine SWNTs and 219 ppm upfield or downfield from a centerband for the functionalized SWNTs). Each spectrum was obtained with a 4.5-μs 90° ^{13}C pulse and a 32.9-ms, proton-decoupled free induction decay (FID), followed by a 180-s relaxation delay for the SWNTs or a 45-s relaxation delay for each of the functionalized SWNTs. In the experiments, we used a total of 1320 scans (66.0 h) for the SWNTs, 7152 scans (89.5 h) for the SWNT-derivative **2a**, 4984 scans (62.3 h) for the SWNT-derivative **2b**, and 3560 scans (44.5 h) for the SWNT amide derivative **3**. Each FID was processed with 50 Hz (1 ppm) of line broadening. The resulting spectrum was phase corrected. A fourth-order polynomial was then applied to the baseline over the region from δ315 to δ−70 to create a nearly flat baseline after the polynomial was subtracted from the spectrum. With much more of the functionalized C_{60} sample, C_{60}-$\{CH_2CH_2COOH\}_n$, available,[24a] a 7-mm OD rotor could be used, which was spun at 7.0 kHz. The spectrum was obtained with a 3.8-μs 90° ^{13}C pulse and a 32.9-ms, proton-decoupled FID, followed by either a 15-s relaxation delay (10 440 scans, 43.6 h) or a 45-s relaxation delay (2132 scans, 26.7 h) to make a rough determination of the relative relaxation rates of the various types of carbons. $^{1}H-^{13}C$ cross polarization/magic angle spinning (CPMAS) spectra of acid acyl peroxides **1a** and **1b** were quickly obtained with 5 kHz MAS, a 1-ms contact time, 32.9-ms FID, and 5-s relaxation delay. ^{13}C chemical shifts are relative to the carbonyl carbon of glycine at 176.5 ppm.[24b]

Results and Discussion

Reactions of SWNTs with Peroxides 1a and 1b. As compared to the fullerenes, particularly C_{60}, the SWNTs are significantly less reactive due to the much lower curvature of their sidewalls built of graphene cylinders. For this reason, the SWNTs require a much longer reaction time (days vs hours) for addition of acyl peroxide-generated free radicals to achieve significant sidewall derivatization, as we observed in our recent studies of several peroxides.[10,24a] In the present work, the carboxyalkyl radicals were thermally produced from dicarboxylic acid acyl peroxides **1a** and **1b** (Scheme 1), which have half-lives of 1 h at 90 °C according to information from Atofina Chemicals. On the basis of that, this particular temperature was chosen for conducting the SWNT functionalization reactions. Because of the inductive effect of the carboxyl group, the reactivity of these carboxyalkyl radicals toward SWNTs was somewhat reduced as compared to undecyl and phenyl radicals, studied earlier.[10,24a] Therefore, in this work, we used a larger excess of the peroxide precursor relative to SWNT (∼10:1 weight ratio) to facilitate the addition reaction (Scheme 1).

Characterization of SWNT Derivatives by Optical Spectroscopy. Raman spectroscopy has proven to be an important tool for characterization of both pristine SWNTs and their sidewall-functionalized derivatives. In the Raman spectrum of purified SWNTs (Figure 1A), the tangential mode at 1594 cm^{-1} is the dominant feature. The bands of the radial breathing mode at 213, 230, and 265 cm^{-1} indicate the diameter distribution of

(23) Clover, A. M.; Houghton, A. C. *Am. Chem. J.* **1904**, *32*, 55.

(24) (a) Reverdy, P.; Peng, H.; Khabashesku, V. N.; Margrave, J. L. *Rice Quantum Institute Sixteenth Annual Summer Research Colloquium*; August 9, 2002; Abstr. p 19. (b) Hayashi, S.; Hayamizu, K. *Bull. Chem. Soc. Jpn.* **1991**, *64*, 685.

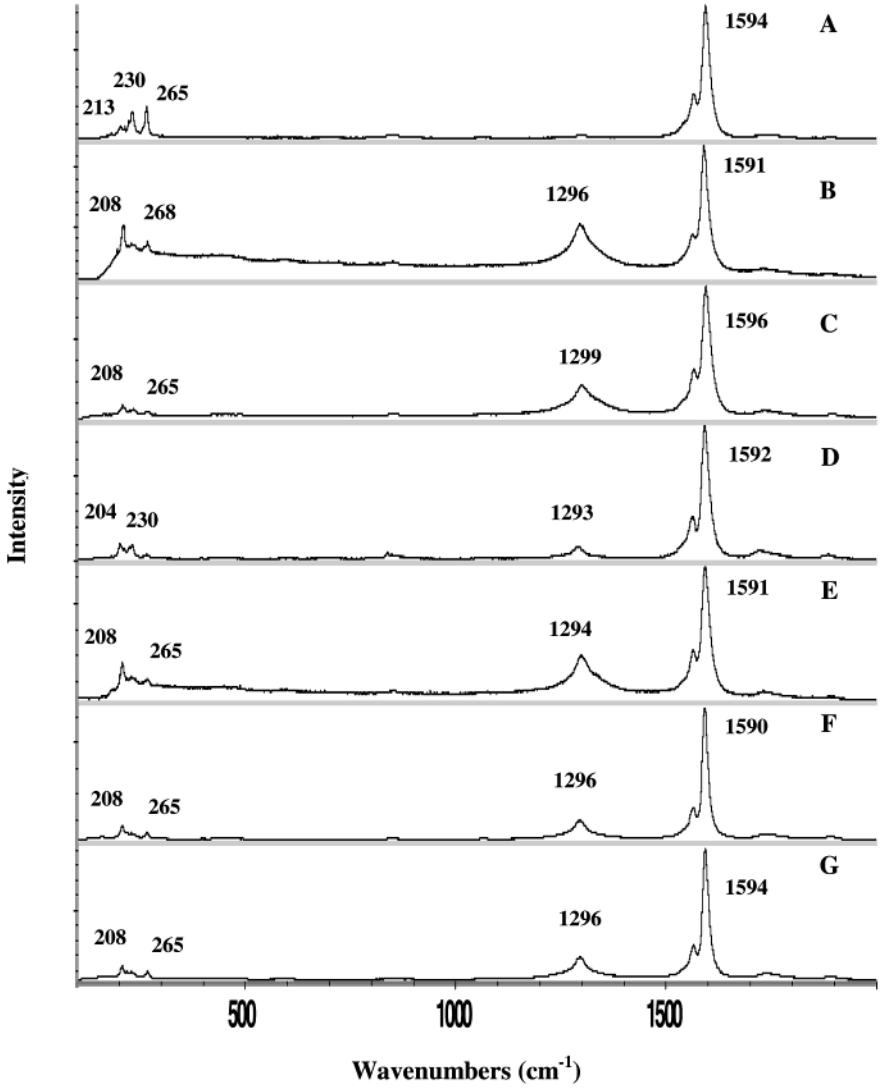

Figure 1. Raman spectra of SWNT materials: (A) pristine SWNTs, (B) **2a**, (C) **2b**, (D) SWNT residue after TGA of **2a**, (E) **3**, (F) **4**, (G) **5**.

HiPco SWNTs. When the sidewalls of the SWNTs are covalently modified, as in the case of SWNT-$\{CH_2CH_2COOH\}_x$ (**2a**), the appearance of a prominent Raman peak at ~1296 cm^{-1} (Figure 1B) due to the sp^3 states of carbon demonstrates the disruption of the aromatic system of π-electrons, as established previously.[2,3,15] The breathing mode bands become weakened in this spectrum, probably because the functional groups attached to the sidewalls hinder the radial breathing oscillation motion.

It should be noted that Raman bands at 265 and 230 cm^{-1} were observed to weaken most with respect to other peaks, which can be explained by a higher reactivity of smaller diameter SWNTs. The Raman features of SWNT-$\{CH_2CH_2CH_2COOH\}_x$ (**2b**) (Figure 1C) are similar to those of **2a** (Figure 1B) except for a slightly lower intensity of the sp^3 mode. This can be related to a somewhat lower number of covalent attachments created on the sidewall surface of **2b** as compared to **2a**.

The modification of the sidewalls in **2a** was also evident in the UV−vis−NIR absorption spectra (Figure 2) from the complete loss of the van Hove band structure typical for pristine SWNTs. The spectrum of the SWNT derivative **2b** was similar to that of **2a**, shown in Figure 2B, indicating a significant alteration of the electronic properties of the nanotubes through sidewall functionalization.

Heating the functionalized SWNTs **2a** and **2b** in argon to 800 °C at the rate of 10 °C/min in a TGA system dramatically reduced the intensity of the sp^3 carbon mode in the Raman spectrum of the nanotube material collected after pyrolysis (Figure 1D). These data indicate that defunctionalization of **2a** and **2b** takes place upon heating, which is in accord with previous data on thermal degradation properties of other sidewall-functionalized SWNTs.[5b,6,7,10] The smaller diameter (less than 1 nm) nanotube derivatives are probably getting "unzipped" under 700−800 °C, which could explain why the Raman peak of the radial breathing mode at 265 cm^{-1} did not recover in the spectrum of **2a** after TGA.

Although the infrared spectra of pristine SWNTs are featureless, FTIR spectroscopy using the ATR accessory is very informative for studying the functional groups attached to the sidewalls of the SWNTs. Figure 3A shows the infrared spectrum of the SWNT-derivative **2a**. The peaks in the 2800−3050 cm^{-1} region are characteristic of C−H stretches, and the broad shoulder band in the 3100−3600 cm^{-1} region is characteristic

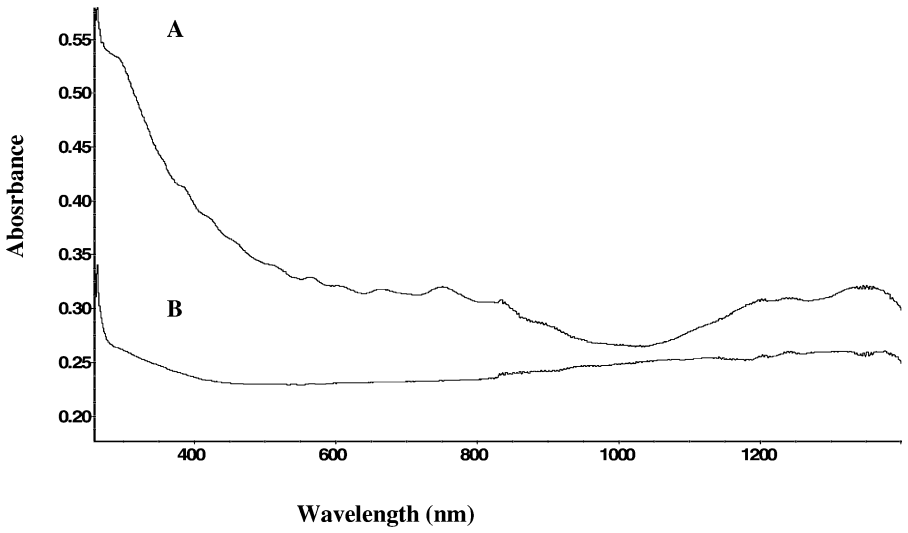

Figure 2. UV−vis−NIR spectra of (A) pristine SWNTs and (B) SWNT derivative **2a**.

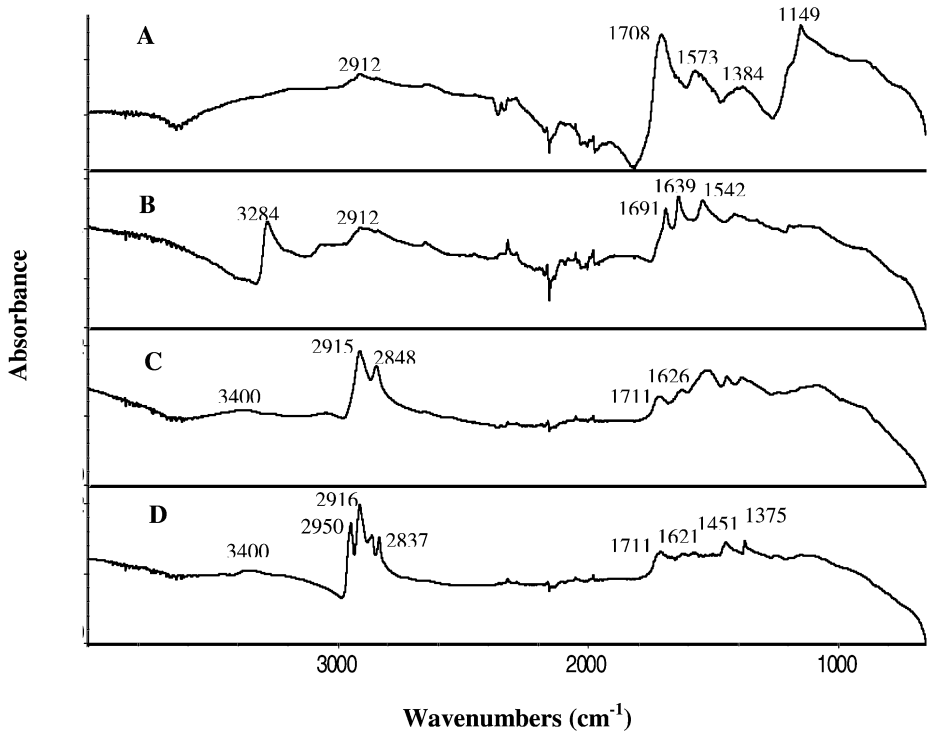

Figure 3. ATR-FTIR spectra of functionalized SWNTs: (A) **2a**, (B) **3**, (C) **4**, (D) **5**.

of acid O−H stretches. The dominant peak at 1708 cm^{-1} can be clearly assigned to the acid carbonyl stretching mode. The broad band at 1384 cm^{-1} can be identified as the C−H bending mode, and a broad peak at 1149 cm^{-1} is identified as the C−O stretching mode. A similar infrared spectrum was obtained for the carboxypropyl derivative **2b**.

The functionalized SWNTs **2a** and **2b** can further react with thionyl chloride and terminal diamines to form the corresponding amides (Schemes 2−4), thus providing chemical evidence for the presence of carboxylic acid groups in the side chain. These reactions were carried out in analogy with the known chemistry of the carboxylic acid groups created on the open ends of SWNTs by oxidizing treatment.[13−15] In the FTIR spectrum (Figure 3B) of the SWNT-$\{CH_2CH_2CONHCH_2CH_2NH_2\}_x$ (**3**), a new intense peak at 3284 cm^{-1} can be assigned to the N−H stretching mode of the amide moiety. The carbonyl peak in **3** shifts to 1691 cm^{-1} (as compared to 1708 cm^{-1} for **2a**) as a result of the peptide C(═O)NH linkage formation. The latter is also characterized by the in-plane amide NH deformation mode observed at 1542 cm^{-1}. The other prominent peak at 1639 cm^{-1} can be assigned to the NH_2 scissoring mode in **3**. The C−H stretchings in **3** are only slightly enhanced as compared to **2a** (Figure 3A).

The SWNT-derivative **2b** was also found to be readily converted into the amide derivative **4** by $SOCl_2$ and 4,4′-methylenebis(cyclohexylamine) treatment at room temperature in accordance with Scheme 3. In the infrared spectrum of **4** (Figure 3C), the features of the methylene C−H stretches at 2915 and 2848 cm^{-1} appear greatly enhanced. The peak at 1711 cm^{-1} and a broad band at ∼3400 cm^{-1} are assigned to the C═O

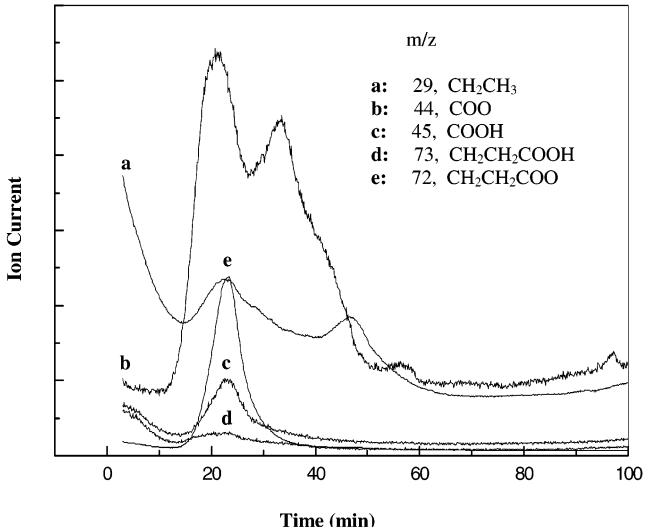

Figure 4. Ion current versus time (temperature) plots obtained for ions (**a**−**e**, *m*/*z*) detected in the course of TG-MS analysis of evolution products from SWNT-derivative **2a**.

and N−H stretching modes, respectively. The NH_2 scissor motion can be most likely associated with the peak observed at 1626 cm^{-1}.

In contrast, **2b** gave only negligible signs of reaction with diethyltoluenediamine at room temperature. However, the amidation reaction (Scheme 4) did occur upon heating at 120 °C, yielding the amide product **5**, whose infrared spectrum is shown in Figure 3D. The bands at 2950 and 2867 cm^{-1} as well as those at 2916 and 2837 cm^{-1} can be assigned to the CH stretches of the CH_3 and CH_2 groups, respectively. The peaks of the carbonyl stretching mode at 1711 cm^{-1} and the NH stretching mode at ∼3400 cm^{-1} again appear weak. The bands at 1621, 1451, and 1375 cm^{-1} can be assigned to the NH_2 scissor, CH deformation, and phenyl ring modes, respectively.[25]

The SWNT derivatives **3**−**5** show characteristic peaks in the Raman spectra (Figure 1E−G) similar to carboxyalkyl SWNTs **2a** and **2b**. This confirms that the reactions of **2a** and **2b** with terminal diamines result in the chemical modification of their side-chain moieties and not the sidewalls.

Thermal Gravimetry/Mass Spectrometry Analysis. Additional evidence for covalent attachment of carboxyalkyl groups to the SWNTs was provided by thermal degradation analyses (TGA) of **2a** and **2b** in the 50−800 °C range coupled with on-line monitoring of the volatile products by a mass spectrometer. These experiments were carried out with 15 mg of **2a** or **2b** placed in a TGA pan and heated at 10 °C/min up to 800 °C in a flow of argon. Figure 4 presents the ion current versus time curves for parent and fragment ions originating from the evolution products detaching from the side chains of SWNT-derivative **2a**.

The evolution curves were obtained for the parent ion (*m*/*z* 73) of the detaching CH_2CH_2COOH radical and for the fragment ions with the *m*/*z* 72 {CH_2CH_2COO}, *m*/*z* 45 {COOH}, *m*/*z* 44 {CO_2}, and *m*/*z* 29 {CH_3CH_2}. All curves for the fragment ions were observed to peak at the same time (evolution temperature) as the evolution curve for the parent ion, which indicates that all fragments originate from the same parent (molecular) ion. The detected fragment evolutions started at about 170 °C, which is comparable to that for methylated, butylated, and hexylated SWNTs (∼160 °C) and is relatively low as compared to phenylated SWNTs (∼250 °C).[15,16] We assume that all of the weight loss occurring during fragmentation is due to pyrolysis of the side-chain groups. On the basis of this assumption, we estimate the degree of SWNT sidewall functionalization as one functional group for every 24 nanotube carbons.

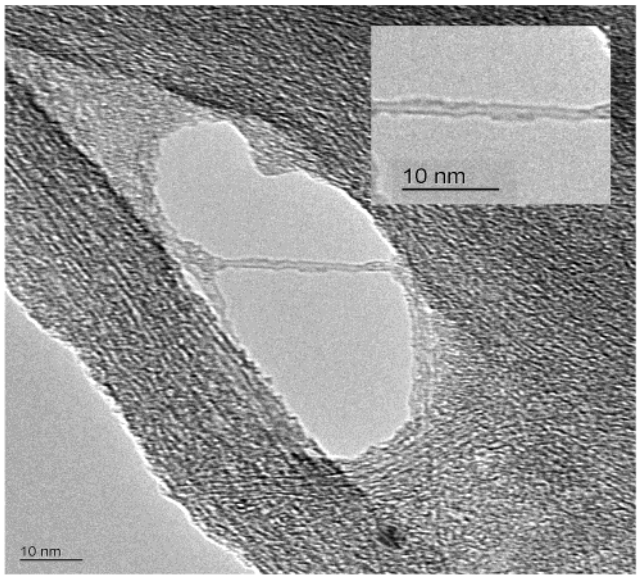

Figure 5. TEM image of the specimen of SWNT-{$CH_2CH_2CONHC_6H_{10}$-$CH_2C_6H_{10}NH_2$}$_x$ (**4**). Inset shows a zoomed-on picture of a single functionalized nanotube.

Microscopy Analysis. Figure 5 shows a typical TEM image of the SWNT derivative **4** specimen placed on lacey carbon-coated copper grid. This image shows that the covalent attachment of functional groups produces a "bumpy" sidewall morphology for the nanotubes of **4** in the bundles observed. A zoomed image of a single nanotube found in the same specimen of **4** (inset in Figure 5) indicates the attached long-chain moieties which tend to bend and stretch along the SWNT sidewalls.

The atomic force microscopy studies of the carboxyalkylated SWNTs **2a** also revealed their predominantly bundled morphology, with the bundle sizes ranging from 10 to 20 nm. Within these bundles, the functionalized nanotubes are most likely held together through intramolecular hydrogen bonds formed by the side-chain terminal carboxylic acid groups.

Solubility. A quantitative comparison of the solubility of pristine SWNTs and the SWNT-derivative **2a** in several polar solvents was performed as follows: 25 mg of SWNT material was dispersed in 200 mL of the selected solvent by sonication for 2 h; the dispersion was left to settle for 48 h; then the decanted top 150 mL of the solution was filtered; and the precipitate collected from the filter was weighed. The solubility data obtained (Table 1) show that, as compared to the pristine nanotubes, the solubility of functionalized SWNTs **2a** is significantly improved. Isopropyl alcohol was found to be the best solvent for SWNT-derivative **2a**.

The photographs in Figure 6 clearly show the great solubility difference between pristine nanotubes and SWNT-derivative **2a** in isopropyl alcohol. However, the functionalized SWNTs were not sufficiently soluble to allow useful solution state ^{13}C NMR

(25) Lin-Vien, D.; Colthup, N. B.; Fatelley, W. G.; Grasselli, J. G. *The Handbook of Infrared and Raman Characteristic Frequencies of Organic Molecules*; Academic Press Inc.: San Diego, CA, 1991; p 299.

Table 1. Solubility Data (mg) for Pristine SWNT and SWNT-Derivative **2a**

solvent, 150 mL	pristine SWNT	SWNT-{CH_2CH_2COOH}$_x$ (**2a**)
o-dichlorobenzene	3.5	7.0
isopropyl alcohol	not soluble	16.0
water	not soluble	15.2
1% NH_4OH in water	not soluble	15.1

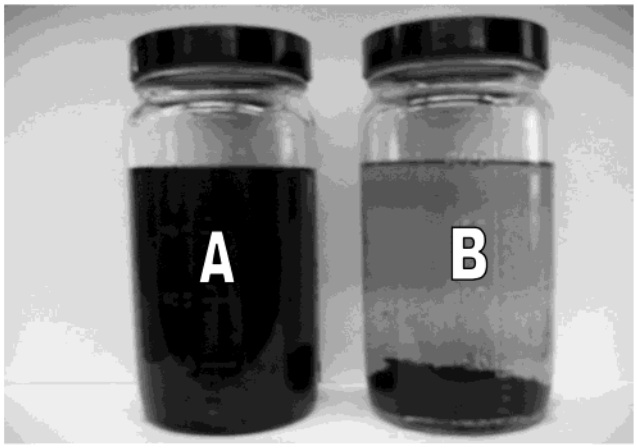

Figure 6. Photographs ofthe SWNT materials dispersed in isopropyl alcohol: (A) acid-functionalized SWNT **2a**, (B) pristine SWNTs.

spectra to be obtained. Therefore, we have carried out these studies in the solid state.

Solid State ^{13}C NMR Studies. Solid state ^{13}C NMR studies have been done by several research groups to further characterize both pristine nanotubes and their derivatives. These reports have dealt with the ^{13}C spin−lattice relaxation behavior of MWNTs,[26b,27] functionalized MWNTs,[28] SWNTs,[29,30d−f] and lithium-intercalated SWNTs;[29c] the ^{1}H spin−spin relaxation behavior of functionalized MWNTs;[28] and the chemical environment of nanotubes[26,27,29b,30a,d−f] and their oxidized (carboxyl-substituted) derivatives before and after heating.[28,30a,e,f] In addition, the calculated ^{13}C chemical shift anisotropy tensors of metallic and semiconductor SWNTs have been reported.[30b,c,e,f] These papers indicate that five different samples of SWNTs give an isotropic ^{13}C NMR signal at δ121−126,[29b,30a,d−f] while

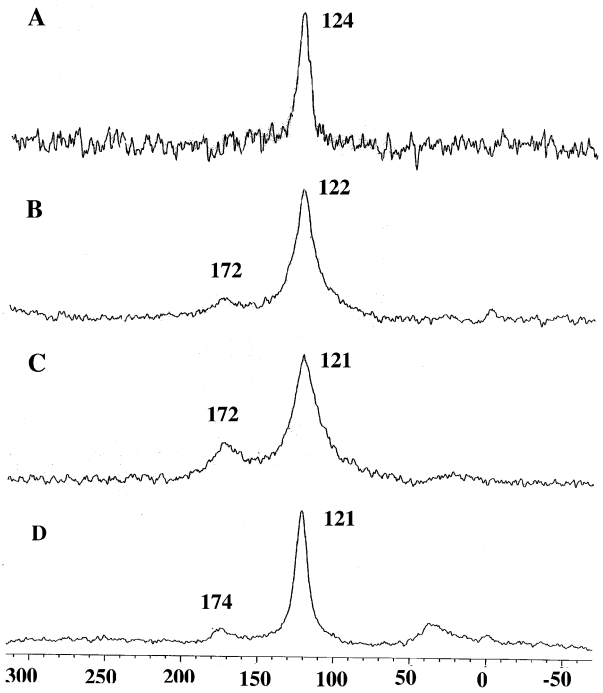

Figure 7. MAS ^{13}C NMR spectra of SWNTs: (A) pristine, (B) **2b**, (C) **2a**, (D) **3**.

three different samples of MWNTs give a considerably broader isotropic ^{13}C NMR signal at δ121−130.[27,31,32] Thus, the observation of an isotropic ^{13}C NMR signal at δ123 for the purified HiPco SWNTs is reasonable (Figure 7A).

However, this signal is considerably narrower (half-height line width is only about 9 ppm) than those observed previously, which suggests that the purified HiPco SWNTs have at least one of the following attributes: more uniform composition (with respect to diameter, length, and chirality) and packing of the tubes into bundles, relatively low metal content, or relatively few defects.

Functionalization with the $(CH_2)_nCOOH$ moieties ($n = 2$ or 3) creates different local environments on the nanotube and clearly broadens this signal (Figure 7B and C). The peak maximum also appears to shift slightly upfield. The Raman (Figure 1B and C), UV−vis−NIR (Figure 2), and IR (Figure 3A) spectra of **2a** and **2b** provide clear evidence for the attachment of aliphatic functionality to SWNT sidewalls, but the methylene groups give very weak signals at best in the MAS ^{13}C NMR spectra. If the corresponding ^{1}H NMR signal is very broad and shifted, decoupling may not be effective, because it would cause the methylene carbon signals to be severely broadened. Additional studies are planned to probe this further.

Functionalization also results in the appearance of a carbonyl signal at about δ172, which is exceptionally shielded for a carboxylic acid.[33] Such a ^{13}C chemical shift is more typical of an ester or anhydride, but the IR absorption at 1708 cm^{-1} (Figure 3A) is clearly more consistent with a carboxylic acid. Furthermore, acid treatment, which would be expected to hydrolyze an ester or anhydride, did not affect this IR peak. Not only is

(26) (a) Maniwa, Y.; Sato, M.; Kume, K.; Kozlov, M. E.; Tokumoto, M. *Carbon* **1996**, *34*, 1287. (b) Maniwa, Y.; Hayashi, M.; Kumazawa, Y.; Tou, H.; Kataura, H.; Ago, H.; Ono, Y.; Yamabe, T.; Tanaka, K. *AIP Conf. Proc.* **1998**, *442 (Electronic Properties of Novel Materials—Progress in Molecular Nanostructures)*, 87.
(27) Kishinevsky, S.; Nikitenko, S. I.; Pickup, D. M.; van-Eck, E. R. H.; Gedanken, A. *Chem. Mater.* **2002**, *14*, 4498.
(28) Xu, M.; Huang, Q.; Chen, Q.; Guo, P.; Sun, Z. *Chem. Phys. Lett.* **2003**, *375*, 598.
(29) (a) Tang, X.-P.; Kleinhammes, A.; Shimoda, H.; Fleming, L.; Bennoune, K. Y.; Bower, C.; Zhou, O.; Wu, Y. *Mater. Res. Soc. Symp. Proc.* **2000**, *593 (Amorphous and Nanostructured Carbon)*, 143. (b) Tang, X.-P.; Kleinhammes, A.; Shimoda, H.; Fleming, L.; Bennoune, K. Y.; Sinha, S.; Bower, C.; Zhou, O.; Wu, Y. *Science* **2000**, *288*, 492. (c) Zhou, O.; Shimoda, H.; Gao, B.; Oh, S.; Fleming, L.; Yue, G. *Acc. Chem. Res.* **2002**, *35*, 1045.
(30) (a) Goze-Bac, C.; Holzinger, M.; Jourdain, V.; Latil, S.; Aznar, R.; Bernier, P.; Hirsch, A. *Mater. Res. Soc. Symp. Proc.* **2001**, *633 (Nanotubes and Related Materials)*, A11.2.1−A.11.2.6. (b) Latil, S.; Goze Bac, C.; Bernier, P.; Henrard, L.; Rubio, A. *Mater. Res. Soc. Symp. Proc.* **2001**, *633 (Nanotubes and Related Materials)*, A14.13.1−A14.13.6. (c) Latil, S.; Henrard, L.; Goze Bac, C.; Bernier, P.; Rubio, A. *Phys. Rev. Lett.* **2001**, *86*, 3160. (d) Goze Bac, C.; Latil, S.; Vaccarini, L.; Bernier, P.; Gaveau, P.; Tahir, S.; Micholet, V.; Aznar, R.; Rubio, A.; Metenier, K.; Beguin, F. *Phys. Rev. B* **2001**, *63*, 100302-1. (e) Goze Bac, C.; Bernier, P.; Latil, S.; Jourdain, V.; Rubio, A.; Jhang, S. H.; Lee, S. W.; Park, Y. W.; Holzinger, M.; Hirsch, A. *Curr. Appl. Phys.* **2001**, *1*, 149. (f) Goze-Bac, C.; Latil, S.; Lauginie, P.; Jourdain, V.; Conard, J.; Duclaux, L.; Rubio, A.; Bernier, P. *Carbon* **2002**, *40*, 1825.
(31) Rao, C. N. R.; Govindaraj, A.; Satishkumar, B. C. *Chem. Commun.* **1996**, 1525.
(32) Tang, B. Z.; Xu, H. *Macromolecules* **1999**, *32*, 2569.

the carbonyl signal at δ172 exceptionally shielded, it also is much broader than the carboxyl signals in the CPMAS spectra of the precursor peroxides. Thus, the π-system of the nanotube itself appears to exert a significant shielding and broadening effect on the carbonyl carbon of the substituent.

There is a precedent for such an effect in solid state ^{13}C NMR and especially in solution state ^{1}H and ^{19}F NMR spectra of functionalized nanotubes. In the ^{1}H−^{13}C CPMAS spectrum of a MWNT bearing $CONH(CH_2)_{17}CH_3$ substituents, the signals for the two CH_2 groups closest to the nanotube were broadened beyond detection.[28] ^{1}H NMR has been used to see the interaction between the substituent and the SWNT.[34a] The signals of the protons next to the nanotube sidewalls are shifted upfield in correlation with the distance from the sidewall of the SWNT functionalized with the aziridino substituent $>N-CO-O-CH_2CH_2-(OCH_2CH_2)_n-CH_2CH_2CH_2CH_3$, and those signals are also broadened.[34b] The same phenomenon has been observed in the ^{1}H NMR spectrum of a SWNT functionalized with a carbene.[34c] A recent report on other aziridino-substituted SWNTs also indicates that the ^{1}H NMR signals are shifted upfield and broadened in the functionalized SWNT.[9b] In the ^{19}F NMR spectrum of a SWNT bearing *n*-C_8F_{17} substituents, the signals for the two CF_2 groups closest to the nanotube are broadened beyond detection.[9a] Finally, in 2D NMR spectra of a SWNT coupled to a bioactive peptide, a decrease and a broadening of the signal intensities were observed for the amino acid residues approaching the aromatic tube walls.[8c]

Broadening and shifting of resonances has also been observed for noncovalently functionalized nanotubes. The major interaction between a *n*-$C_{10}H_{21}O$-substituted poly(*p*-phenyleneethynylene) and a SWNT is believed to be π-stacking; the signals for the methylene protons closest to the SWNT are broadened and shifted upfield by 0.5 ppm, while the phenylene protons are too broad to be detected.[35a] Similarly, π-stacking between a pyrene derivative and a SWNT has also been proposed to explain the small upfield shift of the pyrenyl protons.[35b] In an example where a polymer, a *n*-$C_8H_{17}O$-substituted poly(*m*-phenylenevinylene), wraps around the SWNT, $\pi-\pi$ interactions are believed to be responsible for the broadening and shifting of resonances.[35c] Broadening is particularly noticeable for the aromatic and vinyl protons of the polymer backbone and the protons of the octyloxy chains closest to the aromatic groups; the intensity of these methylene protons is also greatly reduced relative to the intensity of the more remote protons. In another polymer-wrapped SWNT, the poly(vinylpyrrolidone) polymer gives no detectable ^{1}H NMR signals,[35d] while in an example where a $-CH_2NH_2$-substituted crown ether interacts with carboxyl groups on the SWNT, the methylene side-chain resonances are broadened to the point of almost disappearing.[35e] As compared to these illustrative examples of relatively large molecules interacting with (e.g., wrapping around) SWNTs, it is hard to imagine how small, carboxyl-substituted free radicals could do so.

The broadening and shifting of resonances is consistent with experimental[36a,b] and theoretical[36c,d] work indicating a large diamagnetic susceptibility resulting from delocalized electrons (a π-electron ring current) in nanotubes. While C_{60} has five-membered rings with paramagnetic (also called paratropic[37]) ring currents,[38] perfect SWNTs do not have five-membered rings in their sidewall framework, although such rings can be present as defects. The absence of such rings could reasonably be expected to lead to a larger diamagnetic susceptibility.[36a] That the resonances of substituents become more shielded would also be consistent with the presence of diamagnetic (also called diatropic[37]) ring currents in the network of six-membered rings in nanotubes. The ^{1}H NMR spectrum of the fulleroid $C_{61}H_2$, a methanoannulene, provides a classic example of the sensitivity of substituent chemical shifts to the local magnetic field.[39a] (In this case, the proton above a five-membered ring is deshielded by its paratropic ring current, while the proton above a six-membered ring is shielded by its diatropic ring current.[37,38a,39b]) Clearly, much work remains to be done to gain a better understanding of the effects of the substantial diamagnetic susceptibility of functionalized nanotubes on the acquisition, appearance, and interpretation of NMR spectra, particularly in the solid state.

Thus, it is not unreasonable to observe in the spectra of **2a** and **2b** that the signals of the methylene carbons, which are even closer than the carbonyl carbon to the nanotube, are shifted even further upfield and broadened almost beyond detectability. For the sample of **2a**, a very weak broad signal consistent with aliphatic carbon is centered at about δ20, while for **2b**, signals from aliphatic carbons are essentially undetectable, presumably because less derivatization occurred, as indicated in the Raman spectra of **2a** and **2b** (Figure 1B and C).

SWNTs can be sidewall functionalized with long-chain *n*-alkyl (e.g., *n*-$C_{11}H_{23}$[10]) or $(CH_2)_nCOOH$ groups, and a MAS ^{13}C NMR spectrum could be obtained under quantitative conditions. In a direct ^{13}C pulse experiment with a sufficiently long relaxation delay,[28] the integrated intensity of the distinctive methyl signal or carboxyl signal relative to the integrated area of the methylene signals would then indicate the number of methylene carbon signals that had not been detected. Such an

(33) Relevant carboxyl ^{13}C chemical shift data on model compounds with $C_{quat}-CH_2CH_2COOH$, $C_{quat}-CH_2CH_2CH_2COOH$, or similar groups include: (a) 4,4-dimethylhexanoic acid, δ180.6 in $CDCl_3$ relative to TMS: Aurell, M. J.; Domingo, L. R.; Mestres, R.; Muñoz, E.; Zaragozá, R. J. *Tetrahedron* **1999**, *55*, 815. (b) 4,4,6-trimethylheptanoic acid, δ180.5 in $CDCl_3$ relative to TMS: Katritzky, A. R.; Zhang, S.; Hussein, A. H. M.; Fang, Y.; Steel, P. J. *J. Org. Chem.* **2001**, *66*, 5606. (c) 5,5-dimethylhexanoic acid, δ180.3: Taber, D. F.; Ruckle, R. E., Jr. *J. Am. Chem. Soc.* **1986**, *108*, 7686. (d) 5,5-diphenylpentanoic acid, δ179.9 in $CDCl_3$ relative to TMS: Foubelo, F.; Lloret, F.; Yus, M. *Tetrahedron* **1992**, *48*, 9531.

(34) (a) Holzinger, M.; Hirsch, A.; Hennrich, F.; Kappes, M. M.; Dziakova, A.; Ley, L.; Graupner, R. *AIP Conf. Proc.* **2002**, *633 (Structural and Electronic Properties of Molecular Nanostructures)*, 96. (b) Abraham, J.; Hirsch, A.; Hennrich, F.; Kappes, M.; Dziakova, A.; Graupner, R.; Ley, L. *AIP Conf. Proc.* **2002**, *633 (Structural and Electronic Properties of Molecular Nanostructures)*, 92. (c) Holzinger, M.; Hirsch, A.; Bernier, P. *AIP Conf. Proc.* **2001**, *591 (Electronic Properties of Molecular Nanostructures)*, 337.

(35) (a) Chen, J.; Liu, H.; Weimer, W. A.; Halls, M. D.; Waldeck, D. H.; Walker, G. C. *J. Am. Chem. Soc.* **2002**, *124*, 9034. (b) Nakashima, N.; Tomonari, Y.; Murakami, H. *Chem. Lett.* **2002**, 638. (c) Star, A.; Stoddart, J. F.; Steuerman, D.; Diehl, M.; Boukai, A.; Wong, E. W.; Yang, X.; Chung, S.-W.; Choi, H.; Heath, J. R. *Angew. Chem., Int. Ed.* **2001**, *40*, 1721. (d) O'Connell, M. J.; Boul, P.; Ericson, L. M.; Huffman, C.; Wang, Y.; Haroz, E.; Kuper, C.; Tour, J.; Ausman, K. D.; Smalley, R. E. *Chem. Phys. Lett.* **2001**, *342*, 265. (e) Kahn, M. G. C.; Banerjee, S.; Wong, S. S. *Nano Lett.* **2002**, *2*, 1215.

(36) (a) Wang, X. K.; Chang, R. P. H.; Patashinski, A.; Ketterson, J. B. *J. Mater. Res.* **1994**, *9*, 1578. (b) Ramirez, A. P.; Haddon, R. C.; Zhou, O.; Fleming, R. M.; Zhang, J.; McClure, S. M.; Smalley, R. E. *Science* **1994**, *265*, 84. (c) Lu, J. P. *Phys. Rev. Lett.* **1995**, *74*, 1123. (d) Haddon, R. C. *Nature* **1997**, *388*, 31.

(37) Bühl, M.; Hirsch, A. *Chem. Rev.* **2001**, *101*, 1153.

(38) (a) Pasquarello, A.; Schlüter, M.; Haddon, R. C. *Science* **1992**, *257*, 1660. (b) Haddon, R. C. *Science* **1993**, *261*, 1545. (c) Pasquarello, A.; Schlüter, M.; Haddon, R. C. *Phys. Rev. A* **1993**, *47*, 1783. (d) Haddon, R. C. *Nature* **1995**, *378*, 249.

(39) (a) Suzuki, T.; Li, Q.; Khemani, K. C.; Wudl, F. *J. Am. Chem. Soc.* **1992**, *114*, 7301. (b) Prato, M.; Suzuki, T.; Wudl, F.; Lucchini, V.; Maggini, M. *J. Am. Chem. Soc.* **1993**, *115*, 7876.

analysis would be predicated upon the methyl or carboxyl carbon at the end of the long chain being detected at full intensity because that carbon is far from the nanotube. As a practical matter, this analysis would be easier to do with a long-chain *n*-alkyl substituent than with a long-chain $(CH_2)_nCOOH$ substituent because the much larger chemical shift anisotropy of the carboxyl group would require carefully measuring the intensity of its relatively weak spinning sidebands in addition to the intensity of the centerband.

Comparison of the ^{13}C MAS spectra of SWNT-$\{CH_2CH_2COOH\}_x$ (**2a**) and C_{60}-$\{CH_2CH_2COOH\}_x$ (**6**)[40] shows that the π-system of the nanotube causes more shielding and broadening of the carbonyl carbon signal than does the π-system of C_{60}. In the spectrum of C_{60}-derivative **6**, the carbonyl signal is observed at δ177, only about 3 ppm upfield of that in model compounds.[33] As compared to the π-system of SWNT-derivative **2a**, the π-system in **6** is clearly smaller and curves away from the substituent. In addition, C_{60} exhibits a magnetic susceptibility some 30 times smaller (on a per gram basis) than that of nanotubes.[36a] Thus, less shielding and less broadening of the carbonyl carbon in C_{60}-derivative **6** than in SWNT-derivative **2a** is reasonable. This observation is also consistent with functionalization along the sidewall, rather than at the curved end, of the SWNT. A qualitatively similar effect on chemical shift has been noted on the relative shielding of the pyrrolidine protons generated when C_{60} and SWNT are subjected to the same 1,3-dipolar cycloaddition of azomethine ylides.[8a] It is not obvious how one would differentiate $-(CH_2)_nCOOH$ functionalization of an isolated defect site in a SWNT from such functionalization of a long intact π-system, as the carbonyl carbon could be far enough from the defect site to feel the effect of a π-electron ring current near the carbonyl carbon.

Functionalization of the SWNTs with $CH_2CH_2CONHCH_2CH_2NH_2$ groups has surprisingly little effect on the line width of the signal from the nanotube carbons in the spectrum of SWNT-derivative **3** (Figure 7D). The amide group gives a signal at δ174. Signals from the methylene carbons are clearly stronger than in the spectra of **2a** and **2b**. The increased intensity presumably results from the relatively remote $NHCH_2CH_2NH_2$ methylene carbons, whose signals appear upfield of what might be expected.

(40) Peng, H.; Margrave, J. L.; Khabashesku, V. N.; Alemany, L. B., unpublished results.

Finally, even after one takes into account the small number of scans with a long relaxation delay for the purified SWNTs **1**, their spectrum exhibits (Figure 7A) a relatively low S/N as compared to the derivatized SWNTs **2b**, **2a**, and **3** (Figure 7B−D). The relatively low S/N for **1** is consistent with the relatively long ^{13}C T_1 values attributed to semiconducting SWNTs.[29,30e,f]

Conclusion

We have developed an efficient one-step method for covalent attachment of alkyl groups terminated with a carboxylic acid to the sidewalls of carbon nanotubes. The procedure utilizes easily accessible diacyl peroxides containing terminal carboxylic acid groups. Further functionalization of the carboxyl groups on the nanotube side chains with terminal amines and diamines has been demonstrated. These types of sidewall functionalizations impart improved solubility and processing to the nanotubes, which may enable their incorporation into polymer composite materials through chemical bonding to the surrounding matrix via terminal functional groups on the nanotubes. These functional groups also provide sites for covalent attachment of biologically active moieties, for example, amino acids, peptides, proteins, and oligonucleotides, to the nanotubes for drug delivery and biosensor applications.

The solid state ^{13}C NMR studies of functionalized nanotubes have shown that the side-chain carbons exhibit a notable broadening and shifting of resonances consistent with experimental and theoretical work indicating a large diamagnetic susceptibility resulting from delocalized electrons (a π-electron ring current) in nanotubes. These effects were found to be stronger than in similarly functionalized C_{60}, where the π-system is clearly smaller and curves away from the substituent. Additional solid state ^{13}C NMR investigations of functionalized nanotubes will clearly be of interest both in fundamental and in applied studies.

Acknowledgment. This work was supported by the Texas Advanced Technology Program and The Robert A. Welch Foundation of Texas. Funding for the 200 MHz spectrometer was provided by the Office of Naval Research (grant N00014-96-1-1146). We thank Mr. Yunxuan Xiao for discussions and assistance in obtaining the solid state NMR data.

JA037746S